Title: Mitochondrial Disruption Occurs Downstream from β-adrenergic Overactivation by Isoproterenol in Differentiated, but not Undifferentiated H9c2 Cardiomyoblasts: Differential Activation of Stress and Survival Pathways

Author: Ana F. Branco Susana F. Sampaio Mariusz R. Wieckowski Vilma A. Sardão Paulo J. Oliveira

PII: S1357-2725(13)00259-8
DOI: http://dx.doi.org/doi:10.1016/j.biocel.2013.08.006
Reference: BC 4120

To appear in: *The International Journal of Biochemistry & Cell Biology*

Received date: 18-3-2013
Revised date: 19-7-2013
Accepted date: 7-8-2013

Please cite this article as: Branco, A. F., Sampaio, S. F., Wieckowski, M. R., Sardão, V. A., & Oliveira, P. J., Mitochondrial Disruption Occurs Downstream from β-adrenergic Overactivation by Isoproterenol in Differentiated, but not Undifferentiated H9c2 Cardiomyoblasts: Differential Activation of Stress and Survival Pathways, *International Journal of Biochemistry and Cell Biology* (2013), http://dx.doi.org/10.1016/j.biocel.2013.08.006

Mitochondrial Disruption Occurs Downstream from β-adrenergic Overactivation by Isoproterenol in Differentiated, but not Undifferentiated H9c2 Cardiomyoblasts: Differential Activation of Stress and Survival Pathways

Ana F. Branco[1,2], Susana F. Sampaio[1,2,3], Mariusz R. Wieckowski[4], Vilma A. Sardão[1], Paulo J. Oliveira[1*]

1) CNC - Center for Neuroscience and Cell Biology, Largo Marques de Pombal, University of Coimbra, Portugal

2) Department of Life Sciences, Largo Marques de Pombal, University of Coimbra, Portugal

3) Doctoral Programme in Experimental Biology and Biomedicine, Center for Neuroscience and Cell Biology, University of Coimbra, Portugal

4) Department of Biochemistry, Nencki Institute of Experimental Biology, Warsaw, Poland

*to whom correspondence should be sent

Paulo J. Oliveira, Center for Neuroscience and Cell Biology, Largo Marques de Pombal, University of Coimbra, 3004-517 Coimbra, Portugal

Phone: +351 304 502 911

Fax: +351 239 855 789

Email: pauloliv@ci.uc.pt

Abstract:

β-adrenergic receptor stimulation plays an important role in cardiomyocyte stress responses, which may result in apoptosis and cardiovascular degeneration. We previously demonstrated that toxicity of the β-adrenergic agonist isoproterenol on H9c2 cardiomyoblasts depends on the stage of cell differentiation. We now investigate β-adrenergic receptor downstream signaling pathways and stress responses that explain the impact of muscle cell differentiation on hyper-β-adrenergic stimulation-induced cytotoxicity. When incubated with isoproterenol, differentiated H9c2 muscle cells have increased cytosolic calcium, cyclic-adenosine monophosphate content and oxidative stress, as well as mitochondrial depolarization, increased superoxide anion, loss of subunits from the mitochondrial respiratory chain, decreased Bcl-xL content, increased p53 and phosphorylated-p66Shc as well as activated caspase-3. Undifferentiated H9c2 cells incubated with isoproterenol showed increased Bcl-xL protein and increased superoxide dismutase 2 which may act as protective mechanisms. We conclude that the differentiation of H9c2 is associated with differential regulation of stress responses, which impact the toxicity of several agents, namely those acting through β-adrenergic receptors and resulting in mitochondrial disruption in differentiated cells only.

Keywords: isoproterenol; β-adrenergic signaling; apoptosis; mitochondria; H9c2 myoblasts differentiation; reactive oxygen species.

Abbreviations: β-AR, β-adrenergic receptors; ANOVA, analysis of variance; BSA, bovine serum albumin; cAMP, cyclic-AMP; DAPI, 4',6-diamidino-2-phenylindole; $\Delta\Psi$, mitochondrial transmembrane electric potential; DHE, dihydroethidium; DMEM, Dulbecco's-modified eagle's medium; DMSO, dimethyl sulfoxide; DTT, DL-Dithiothreitol, FBS, Fetal bovine serum; HBSS, Hank´s Balanced Salt Solution; ISO, isoproterenol; MAPK, mitogen-activated protein kinases; mPTP, mitochondrial permeability transition pore; NAC, n-acetyl-cysteine; PMSF, phenylmethylsulfonyl fluoride; PVDF, polyvinylidene difluouride; RA, all-trans retinoic acid; ROS, reactive oxygen species; SRB, sulforhodamine B; SOD2, superoxide dismutase 2; TMRM, tetramethylrhodamine methyl ester; CM H_2DCFDA, 5-(and 6)-chloromethyl- 2', 7'-dichlorodihydrofluorescein diacetate

1. Introduction

The chronic exposure of cardiomyocytes to catecholamines is associated with pathologic alterations (Communal et al., 1998). Hyperadrenergic activation of β-adrenergic receptors (β-AR) leads to increased cytosolic calcium overload, production of reactive oxygen species (ROS) (Zhang et al., 2005) and cardiomyocyte apoptosis (Communal et al., 1998), resulting in myocardium deterioration and decompensated heart failure (Diwan and Dorn, 2007). Indeed, the control of myocyte cell loss through the suppression of cell death pathways represents an ideal strategy to prevent cardiodegeneration resulting from excessive β-adrenergic drive.

Mitochondria are key regulators of cellular metabolism. Once mitochondrial function is affected, critical ATP-dependent mechanisms are compromised and mitochondria-induced apoptotic cell death is activated (Chiong et al., 2011). Increased mitochondrial production of ROS play an important role in the regulation of multiple stress and toxicity responses (Afanas'ev, 2011). Assessing stress responses in cardiomyocytes is critical in the understanding of the mechanisms of heart degeneration during different pathologies and in the designing of proper therapies. The present work addresses the mechanisms by which cardiomyoblasts respond to β-AR overstimulation according to their differentiation state. For this objective, we used the rat myoblastic H9c2 cell line, widely used as a surrogate for cardiac cells. Since H9c2 myoblasts differentiate into skeletal and cardiac muscle cells under different culture conditions and since differences exist regarding cell metabolism (Pereira et al., 2011), we aimed at investigating differences in stress signaling pathways and mitochondrial alterations that may render undifferentiated H9c2 cells more resistant to β-adrenergic over-stimulation as previously described (Branco et al., 2011). Our hypothesis is that β-AR over-stimulation by the agonist Isoproterenol (ISO) results in different cell fate depending on the cell

differentiation stage, which is explained by different stress responses resulting from cytosolic calcium accumulation, increased oxidative stress, and mitochondrial alterations. In a follow-up to our previous study (Branco et al., 2011), the objective of the present study is to identify downstream triggers of stress responses and specific mitochondrial alterations resulting from ISO β-AR over-stimulation and which are dependent on the differentiation state of the cells.

2. Materials and Methods

2.1. Reagents

A complete list of reagents and sources is available in the supplementary online material. All reagents used in this work were of the greatest degree of purity commercially available. To prepare solutions, ultrapure distilled water was used in order to minimize contamination with metal ions.

2.2. H9c2 Cell Culture and Differentiation Process

H9c2 cells were cultured and differentiated as described before (Branco et al., 2012, Branco et al., 2011, Pereira et al., 2011, Sardao et al., 2009) (please see supplementary online material). Experiments were conducted in three experimental groups: a) undifferentiated myoblasts in 10% serum media, b) differentiated muscle cells in 1% serum media, and c) differentiated cells in 1% serum media plus 1 μM RA.

2.3. Analysis of Drug Cytotoxicity

Cell density was evaluated by the sulforhodamine B (SRB) assay (Serafim et al., 2008, Houghton et al., 2007). H9c2 cells were seeded in 6- or 24-well plates (35,000 cells/ml), allowed to attach for 1 day and pre-incubated individually with the specific compounds: 30 minutes with 30 μM of pifithrin-alpha, 1 hour with 50 μM of LY294002 or 2 hours with 100 μM NAC, always prior to ISO treatment (24, 48 or 96 hours). The concentration of the compounds used did not cause toxicity in preliminary toxicity assays (data not shown). Vehicle controls were also performed.

2.4. Western Blotting

Specific protein semi-quantization was performed by Western Blotting, as detailed in the online supplementary online.

2.5. Vital Fluorescence of H9c2 Cells by Using Tetramethylrhodaminemethyl-ester (TMRM) and Hoechst 33342

H9c2 cells grown on glass-bottom dishes (35,000 cells/ml) were treated with ISO. Forty-five minutes before incubation time, TMRM (100 nM), Hoechst 33342 (1 mg/ml) or calcein-AM (300 nM) were added to cells at 37°C in the dark. Media was then replaced by Krebs buffer (1 mM $CaCl_2$; 132 mM NaCl; 4 mM KCl; 1.2 mM Na_2HPO_4; 1.4 mM $MgCl_2$; 6 mM glucose; 10 mM HEPES, pH 7.4) supplemented with 10% FBS. Epifluorescence microscopy images were obtained using a Nikon Eclipse TE2000U microscope and were analyzed using Metamorph software (Universal Imaging, Downingtoen, PA). Confocal microscopy images were collected using a Zeiss LSM 510-Meta confocal microscope and analyzed using LSM Image Browser (Zeiss, Germany).

2.6. Vital Fluorescence of H9c2 Cells by Using Mitotracker Red and DAPI

H9c2 cells were seeded in 6-well plates with a glass coverslip per well at a density of 35,000 cells/ml. After 1 day of cell attachment, cells were incubated with 50 μM of LY294002 (phosphoinositide 3-kinases-PI3Ks inhibitor) for 1 hour prior to incubation with 50 or 100 μM of ISO for 24 (for differentiated H9c2 cells) or 48 hours (for undifferentiated cells). Thirty minutes prior the end of the incubation time, cells were incubated with Mitotracker Red (125 nM) at 37°C in the dark, washed with cold PBS,

fixed with ice-cold absolute methanol and stored at -20°C. A mounting solution composed by the anti-fading reagent conjugated with 4',6-diamidino-2-phenylindole (DAPI) was used. Cells were visualized by epifluorescence microscopy using a Nikon Eclipse TE2000U microscope (Nikon, Melville, NY, USA). The UV filter was used for DAPI imaging and the rhodamine filter for Mitotracker Red fluorescence imaging. Images were obtained using Metamorph software (Universal Imaging, Downington, PA).

2.7. Flow Cytometry Analyses of Cytosolic Calcium, Mitochondrial ΔΨ and Superoxide Anion

Subconfluent cells originated from the three groups of H9c2 cells used in this study and cellular preparations after ISO treatment were harvested by trypsinization and centrifugation. The cellular pellet was ressuspended in 500µl of a buffer solution (120mM NaCl; 3.5mM KCl; 0.4mM KH_2PO_4; 20mM HEPES; 5mM $NaHCO_3$; 1.2mM Na_2SO_4 and 10mM pyruvate at pH 7.4, 1.2 mM $MgCl_2$, 1.3mM $CaCl_2$ and 5% FBS) plus the respective probe (2 µM Fluo-4 AM, 100 nM TMRM or 5µM MitoSox Red) in order to evaluate intracellular calcium concentration, mitochondrial transmembrane potential (ΔΨ) and mitochondrial superoxide anion, respectively. Cells were incubated at 37°C in the dark for 30 minutes before the end of treatment with ISO. Cells were then analyzed in a FACScalibur Flow cytometer, using the FL1 or the FL2 filter sets (MitoSox e TMRM fluorescence, respectively) and counted using the cytometer Cell Quest software package.

2.8. Oxidative Stress Measurements

Undifferentiated and differentiated H9c2 cells seeded in 12-well plates and incubated 48 hours with ISO were incubated during 20 min at 37°C in the presence of 0.5 µM dihydroethidium (DHE) in PBS containing 5 mM glucose. Cells were washed twice with PBS, and the fluorescence was recorded in a microplate reader at 535 nm excitation and 635 nm emission wavelengths. Following the same protocol, 2 µM CM-H_2DCFDA was incubated with cells and fluorescence read in a microplate reader at 495 nm excitation and 520 nm emission wavelengths.

2.9. Caspase-3-like Colorimetric Activity Assay

Total cellular extracts were collected by trypsinization and centrifuged twice at 1,000 xg, 4°C during 5 minutes. Floating cells were also collected. The pellet was resuspended in collection buffer (20 mM HEPES/NaOH pH 7.5, 250 mM sucrose, 10 mM KCl, 2 mM $MgCl_2$, 1 mM EDTA) supplemented with 2 mM DTT, 100 µM PMSF and a protease inhibitor cocktail. Cell extracts were disrupted by sonication. Protein concentration was determined by the Bradford assay (Bradford, 1976). Caspase 3-like activity was determined as described before (Sardao et al., 2009) (see supplementary online material).

2.10. Determination of Intracellular cAMP Content

Cyclic AMP content was measured by using a commercial kit (cyclic AMP XP™ assay kit) and by following vendor´s instructions (Cell Signaling). Details are available in the supplementary online material.

2.11. Statistical Analyses

Data analysis was performed by using GraphPad Prism 4.0 program (GraphPad Software, Inc., La Jolla, CA, USA) and data were expressed as means ± SEM for the number of experiments indicated in the legends of the figures. Multiple comparisons were performed using one-way analysis of variance (ANOVA) followed by Dunett test. The t-test was used in proliferation studies to compare two groups. Significance was accepted when p value < 0.05.

3. Results

3.1. Differentiated H9c2 Cells are More Susceptible to ISO Toxicity

As reported before, lowering the serum content in the culture media to 1% led the H9c2 cell differentiation to a phenotype characteristic of adult muscle cells (Branco et al., 2011) (data not shown). Supplementation of the culture media with RA increases the content of cells expressing the specific cardiac marker Troponin I (Branco et al., 2012); the same was observed in our study (data not shown).

As previously demonstrated by us (Branco et al., 2011), 1% FBS + RA presented a lower total amount of β1-AR when compared with the two other cell groups (Fig. 1A), while no inter-group differences were identified for β2-AR content (Fig. 1B), as determined by Western Blotting. The toxicity of ISO on differentiated H9c2 cells (1% FBS and 1% FBS + RA) resulted in mitochondrial membrane depolarization, shown as loss of mitochondrial TMRM labeling (Fig. 1D and 1E). ISO did not result in cellular morphological alterations or loss of TMRM fluorescence in undifferentiated myoblasts (Fig. 1C). When differentiated H9c2 cells were treated with ISO, the number of multi-

nucleated cells present was very low, indirectly suggesting that this type of cells was predominantly affected, as shown before (Branco et al., 2011).

3.2. Differentiated H9c2 Cells Have Increased Cytosolic Calcium after ISO Treatment

One of the important mediators of ISO-induced cell cytotoxicity is the activation of calcium channels, leading to an overload of cytosolic calcium (Minakawa et al., 2003). To verify if basal intracellular calcium depended on the cell differentiation state, we used the calcium-dependent fluorescent probe Fluo-4 AM. H9c2 myoblast differentiation is accompanied by an increase in cytosolic calcium, especially for RA-differentiated cells (Fig. 2A, left), which express cardiomyocyte-specific markers (Pereira et al., 2011). After incubation of the three cellular groups with ISO during 48 hours, a higher intracellular calcium concentration was only found in differentiated H9c2 cells when incubated with 100 μM ISO (data not shown). Nevertheless, we cannot distinguish between ISO/β-adrenergic-induced stimulation of calcium uptake, upstream of several signaling/stress pathways, or as occurring as a downstream consequence of cell death. To determine primary ISO effects on cytosolic calcium, further experiments were performed with 2, 3 and 6 hours of incubation. An increase of intracellular calcium was observed in differentiated cells after 2 hours of incubation with the increase in RA-differentiated cells being significant for 6 hours of incubation time (Fig. 2A). During these shorter incubation times, loss of cells was not observed (data not shown).

Since intracellular levels of cAMP and cellular calcium are related (Zhang et al., 2013), the basal levels of the former were evaluated (Fig. 2B, left). A significant decrease of cAMP intracellular content on RA-differentiated H9c2 cells was found when compared with the undifferentiated group (10% FBS). Interestingly, after incubation with 50 μM

ISO for 48 hours, an increase of cAMP was observed in both differentiated cell groups for the lowest ISO concentration tested (Fig. 2B, right).

3.3. Isoproterenol-induced Mitochondrial Alterations in Differentiated H9c2 Cardiomyoblasts

Our next experimental question was whether ISO toxicity in the different groups of cells involve mitochondrial alterations. This was assessed by three distinct end-points: mitochondrial depolarization, generation of superoxide anion and loss of subunits from the oxidative phosphorylation apparatus. We have previously identified H9c2 differentiation-specific alterations in mitochondrial proteins related with cell survival mechanisms including VDAC, Bax and Bcl-2 (Branco et al., 2011). These proteins regulate apoptotic mitochondrial signaling, suggesting other alterations in mitochondrial physiology may occur after ISO treatment of differentiated cells (Hou and Hsu, 2005).

We initiated by investigating alterations in $\Delta\Psi$ by using the fluorescent probe TMRM under both basal conditions (no ISO treatment, Fig. 3A) as well as after ISO treatment for 1, 3, 6 and 48 hours (Fig. 3B-E). No statistically significant differences in basal conditions (Fig. 3A) or after 1, 3 and 6 hours (Fig. 3B, C and D) incubation with ISO were found between groups. When the treatment was extended to 48h, differentiated H9c2 cells incubated with the lower concentration of ISO showed increased TMRM fluorescence, suggesting increased $\Delta\Psi$. When incubated with the higher ISO concentration for 48 hours, RA-differentiated cells suffered a large decrease in mitochondrial TMRM accumulation (Fig3E).

For measuring mitochondrial superoxide anion, the fluorescent probe MitoSox was used. For this specific protocol, we performed a control with rotenone, a Complex I

inhibitor which leads to superoxide anion production (Marella et al., 2007). This positive control avoided measuring the maximal production of that oxygen-derived species and at the same time, normalizes the results after ISO treatment. Our results show an increase in mitochondrial superoxide anion after cellular differentiation to a cardiac-like phenotype (Fig. 3F). As expected, rotenone (9 μM during 1 hour incubation) increased MitoSox fluorescence in all three groups, although no cell differentiation-related differences were measured after rotenone treatment. The next step was determining whether ISO treatment caused a further increase in MitoSox fluorescence. The results for each control or treatment group were normalized to the maximal fluorescence obtained in the presence of rotenone (as described above). The results obtained showed that ISO treatment for 1 and 3 hours did not cause any measurable increase in MitoSox fluorescence (Figs. 3G and H). A significant increase in MitoSox fluorescence in differentiated H9c2 cells, for both 6 hours (no RA only) and 48 hours (both groups of differentiated cells) was detected (Fig. 3I and J). We also used the fluorescent probes H_2DCFDA, which has been described to be a non-specific ROS probe (Pereira et al., 2012) and DHE, a qualitative reporter of cellular superoxide anion (Benov et al., 1998) to investigate ISO-induced oxidative stress. In accordance, the results indicate an increase in cell fluorescence for both probes when using the highest ISO concentration in the two differentiated cell groups after 48 hours of treatment, although this may be a consequence of the progression of cell death (data not shown).

Furthermore, we investigated whether ISO caused alterations in the machinery responsible for oxidative phosphorylation. An antibody cocktail directed at several proteins involved in energy production including ATP synthase subunit alpha, NADH dehydrogenase (ubiquinone) 1 beta subcomplex subunit 8 (NDUFB8), a subunit from mitochondrial complex I and a 30 kDa subunit of mitochondrial complex II was used

(Fig. 4). Significant decreases in complex II 30kDa subunit and in the nuclear-encoded NDUFB8 subunit in RA-differentiated H9c2 cells were found after treatment with ISO. Although no differences were found in undifferentiated or differentiated cells in the absence of RA, it is noteworthy that a tendency for an increase in all three subunits was found in the former group, with the opposite being present in the latter, except for the ATP synthase subunit (Fig. 4).

3.4. Isoproterenol–induced Alterations in Survival/Death Signaling Pathways

Mitochondrial alterations, including increased global oxidative stress, trigger cell death (Li et al., 2012) or stimulate protective pathways in order to rescue cells. We analyzed three mitochondrial proteins that have an important role on mitochondrial survival/death decisions, including SOD2, the manganese superoxide dismutase isoform (Morten et al., 2006), cyclophilin F (also often described as cyclophilin D) a matrix chaperone involved in the mitochondrial permeability transition (Di Lisa et al., 2011) and Bcl-xL, a Bcl-2 family protein, which inhibits mitochondrial-mediated cell death (Ogata and Takahashi, 2003). The data now obtained shows that ISO, when incubated with H9c2 cells in different stages of differentiation causes an up-regulation of all three proteins in the undifferentiated cell group, while the content in Bcl-xL decreases in the RA-differentiated group (Fig. 5 A-C).

The intracellular content of the multi-role transcription factor and mediator of mitochondrial apoptotic signaling p53 (Zheltukhin and Chumakov, 2010, Fujita and Ishikawa, 2011) was also investigated after incubation with ISO (Fig. 5D). Not unexpectedly, the highest ISO concentration used caused a statistically significant increase only in the differentiated cell groups. No significant differences existed when comparing the three cell groups in terms of basal p53 content (data not shown).

Phosphorylation of p66Shc on serine 36 by protein kinase C beta increases during cellular stress and results in amplifying mitochondrial oxidative stress and apoptotic signaling (Cosentino et al., 2008). ISO increases the ratio between Ser36-phosphorylated p66Shc and the total p66Shc content in the two groups of differentiated cells, as opposed to undifferentiated myoblasts where a small, non-significant increase was observed (Fig. 5E). It is worth mentioning that the total amount of p66Shc was not altered during treatment.

3.5. p53 Inhibition and Antioxidant Supplementation Effects in ISO cytotoxicity

Since p53 is increased after ISO treatment in the two differentiated cell groups (Fig. 5D), we asked whether p53 inhibition by pifithrin-alpha (Zhang et al., 2011) prior to ISO treatment, prevented loss of cells. When pre-incubated with pifithrin-alpha, ISO toxicity was prevented in the two differentiated cell groups (Fig. 6A, middle and right panel). In order to investigate pifithrin-alpha effects on undifferentiated cells incubated with ISO, we extended ISO incubation to 72 hours in order to increase cytotoxicity. As previously described (Branco et al., 2011), loss of cells is minimal for shorter incubation time points. Interestingly, the addition of pifithrin-alpha previous to ISO treatment increased undifferentiated cell loss induced by the latter (Fig. 6A, left).

We have also addressed the role of oxidative stress on ISO-induced toxicity on H9c2 cells in different stages of differentiation. Undifferentiated H9c2 cells were incubated with ISO for 96 hours, while differentiated cells were incubated for 48 hours. N-acetylcysteine (NAC), a precursor for GSH synthesis (Basha and Priscilla, 2013) prevented the loss of cells on differentiated (Fig. 6B, middle and right panels) but not on undifferentiated myoblasts (Fig. 6B, left panel).

3.6. PI3K/Akt and ISO cytotoxicity

To evaluate whether PI3K/Akt signaling plays a significant role on ISO-induced toxicity in the three groups of H9c2 cells, intracellular Akt and its phosphorylated form were assessed by Western Blotting. The results showed no differences regarding total Akt protein content between the three experimental groups (Fig. 7A). Since PI3K/AKT acts as a pro-survival pathway (Wang et al., 2013), it was interesting to observe that the serine 473-phosphorylated (active) form of Akt was increased in RA-differentiated cells when incubated with 100μM of ISO. The role of PI3K/Akt-activated pathway on ISO-induced cell death was further confirmed by the SRB assay. The three cellular experimental groups were incubated with the specific inhibitor of the PI3K/Akt pathway, LY294002 (Sun et al., 2004) for 1 hour prior to ISO treatment. The inhibition of PI3K/Akt pathway by LY294002 increased ISO toxicity in all three groups (Fig. 7B and 7C). This was particularly evident for the undifferentiated group (Fig. 7B). Moreover, confocal microscopy (Fig. 7C) confirmed that LY294002 increased ISO toxicity, seen as loss of cells and by the appearance of condensed nuclear chromatin.

3.7. Activation of Caspase Signaling During ISO-induced Differentiated H9c2 Cell Death.

ISO induces poly(ADP-ribose) polymerase (PARP) cleavage, a specific marker of cell death (Branco et al., 2011). Since PARP is a target for caspase 3 (Chaitanya and Babu, 2009), our current study confirmed the involvement of caspase signaling activation by evaluating the content of the active form (Fig. 8A) and activity (Fig. 8B). For the time point measured (48 hours), a statistically significant increase in caspase 3 active

fragment was detected in cells differentiated with serum reduction only and treated with ISO. No differences were found in the two other groups (Fig. 8A). However, caspase-3-like activity was significantly increased in the differentiated groups.

4. Discussion

Isoproterenol-induced β-adrenergic overload leads to cardiac cell dysfunction, which is a good example of chemically-induced heart toxicity and failure (Nichtova et al., 2012). The use of H9c2 cells, which express β-adrenergic receptors (Fig. 1 and (Branco et al., 2011)) in different differentiation stages allows us to elucidate cell signaling mechanisms that underlie the susceptibility of the developing muscle to β-adrenergic agonists. We previously demonstrated that differentiated H9c2 cells are more susceptible to supra-physiological concentrations of the β-adrenergic agonist ISO, (Branco et al., 2011). The present work moves forward by analyzing differentiation-dependent downstream stress pathways stemming from β-adrenergic activation as well as mitochondrial alterations resulting from ISO treatment in the two populations.

A key mediator of the differences between undifferentiated and differentiated H9c2 cardiomyoblasts regarding ISO toxicity difference may be calcium-mediated downstream activation of signaling pathways, which follows through cAMP/PKA activation (Zhou et al., 2009, Mann et al., 1992). Increased basal calcium has been previously described in several models of cell differentiation, including cardiac cells (Fu et al., 2006), mouse embryonic stem cells (ES) (Metzger et al., 1994), human induced pluripotent stem cells (hiPSCs) (Lee et al., 2011) and rat neonatal cardiomyocytes (Gomez et al., 1994). β-receptor activation modulates L-type calcium channels and ryanodine receptors (RyR) (the major sarcoplasmic reticulum calcium release channels in cardiac and skeletal muscles), as well as sarcoplasmic reticulum (SR) Calcium-

ATPase (SERCA2a), contributing to transient calcium levels signals (Schmidt et al., 1999, Zhou et al., 2009, Leblais et al., 2004). During H9c2 differentiation process, the expression of PKA-regulated cardiac/α_{1C} L-type voltage-dependent calcium channels (LTCCs) increases (Menard et al., 1999). More expressed/active calcium channels in differentiated H9c2 cells may increase the susceptibility to agents that further increase cytosolic calcium, including ISO. Increased calcium may result from hyperactivation of the cAMP/PKA pathway in differentiated H9c2 cells (Harris, 1977), although differentiated H9c2 myoblasts gradually decreased cAMP and AC activity (Pagano et al., 2004), which may serve as adaptation to increased cytosolic calcium during differentiation. Under normal conditions, calcium stimulates mitochondrial metabolism leading to increased NADH and ATP production (Mildaziene et al., 1996). However, calcium overload also leads to mitochondrial dysfunction, increased superoxide anion production, leading to mPTP induction and triggering cell death (Izem-Meziane et al., 2012). In fact, a significant increase in cytosolic calcium is observed after just 2h in low-serum media-grown cells (and after 6h in RA-differentiated cells), preceding any significant alteration of mitochondrial superoxide anion or $\Delta\Psi$. Increased mitochondrial superoxide anion generation in differentiated H9c2 cells (Fig. 3) or global cell oxidative stress (data not shown) may result in mitochondrial damage, consequently leading to decreased $\Delta\Psi$ (Fig. 3) and also to the loss of oxidative phosphorylation subunits (Fig. 4). In fact, it is noticeable that a significant increase in superoxide anion was observed before any alteration in $\Delta\Psi$ (Fig. 3D and 3I). Interestingly, undifferentiated cells show increased MnSOD content after ISO treatment (Fig. 5B), which may act to confer antioxidant protection. Despite increased mitochondrial mitochondrial cyclophylin D (or F, as it is also described (Di Lisa et al., 2011, Giorgio et al., 2010)) content is often associated with increased induction of the mPTP (Halestrap, 2010), since this was

observed in undifferentiated cells only suggests a toxicity response which may protect cells (Fig. 5C). Of note, the intermediate concentration of ISO (50 μM) appears to cause mitochondrial hyperpolarization in differentiated cells after 48 hours of treatment with ISO (Fig. 3E), which may be related with the initial stages of cell death (Zorov et al., 2006). The higher detection of mitochondrial superoxide anion under untreated conditions (Fig. 3F) is in agreement with studies documenting the requirement of redox signaling alterations for myoblast differentiation (Schmelter et al., 2006). Indeed, mitochondria function and ROS generation play a fundamental role in establishing metabolic mechanisms that drive undifferentiated myoblasts to a cardiac-specific energetic requirement during cardiomyogenesis (San Martin et al., 2011, Chung et al., 2007). Although the role of oxidative stress on ISO toxicity on differentiated H9c2 cells was confirmed by the protection afforded by NAC, a GSH up-regulating agent, the same agent was unable to prevent ISO toxicity for longer periods on undifferentiated cells (Fig. 6B). Because a primary increase in global oxidative stress can potentiate the formation of more ROS in multiple cell sites, and because the oxidative stress markers we measured only occurred for the highest concentration of ISO used in differentiated cells (Fig. 3B), the results obtained may be a primary response to an hyperadrenergic state caused by ISO (seen as at early time point, 6 hours) or as a consequence of cell death signaling, which occurs for later time points (48 hours).

The above-referred interplay between calcium and oxidative stress may also regulate other stress pathways involved in cell death or survival including involving p53 and p66Shc. The increase in the transcription factor p53 in differentiated cells (Fig. 5D) appears to be particularly involved in the mechanisms of ISO toxicity since the p53 inhibitor pifithrin-alpha (Zhang et al., 2011), decreased ISO toxicity on differentiated

cells (Fig. 6A, middle and right panels), although increasing the toxicity on undifferentiated cells, when incubated for longer periods with ISO (Fig. 6A, left panel).

Also, p53 activation may have led to increased Bax expression observed after ISO treatment in differentiated cells (Branco et al., 2012). In this case, anti-apoptotic proteins such as Bcl-2 or Bcl-xL may alter the balance between anti- and pro-apoptotic proteins and determine cell survival or death (Rong and Distelhorst, 2008). In fact, altered content in pro and anti-apoptotic was measured in H9c2 cells after DOX treatment ((Branco et al., 2011) and Fig. 5), with undifferentiated cells tilting the balance towards an anti-apoptotic phenotype. Inhibition of the survival pathway PI3K/Akt (Aoyagi and Matsui, 2011), activated during ISO treatment (Fig. 7A), lead to increased cytotoxicity, even on undifferentiated cells (Fig. 7B). The PI3K/Akt inhibits pro-apoptotic Bcl-2 family members such as Bax and Bad (Wang et al., 2013). However, differentiated cells did not show increased levels of anti-apoptotic proteins from the Bcl-2 family such as Bcl-xL and Bcl-2 (Fig. 5A) which can compromise the cooperative action between both PI3K/Akt and Bcl-xL/Bcl-2 pathways, leading to cell protection.

ISO treatment resulted in increased activation of p66Shc Ser36-phosphorylated form (Fig. 5E) in differentiated cells. p66Shc is a protein that regulates oxidative stress responses and apoptosis (Lebiedzinska et al., 2013) and its activation has been described for several toxicants, being considered an intracellular stress response pathway (Carpi et al., 2009), downstream from a source of activation present only in differentiated cells.

Finally, an end-result of ISO toxicity is the increase in apoptotic caspase 3 activation in differentiated cells (Fig. 8) as observed, confirming previous results showing cleavage of Poly (ADP-ribose) Polymerase (PARP), after ISO treatment (Branco et al., 2011).

Our findings show that the maturity of H9c2 cardiac cells is critical on their stress responses to β-adrenergic agonists. Interestingly, differentiated H9c2 cells have a lower content in β_1-AR, as measured by Western Blotting (Fig. 1). Since this sub-type is more associated with pro-apoptotic effect of beta-adrenergic stimulation (Communal et al., 1998), the results obtained in the present and past (Branco et al., 2011) work suggest than more than the total β-AR sub-type content, the downstream activation of stress and survival pathways determines fate for each cell type. Mitochondrial metabolism alters with H9c2 differentiation (Comelli et al., 2011, Pereira et al., 2011). An increase reliance on mitochondrial metabolism for ATP production may also imply a remodeling on mitochondrial stress/toxicity responses which impacts mitochondria responses to foreign stresses. Further identification of the molecular mechanisms that mediate stress/survival/death responses in muscle cells in different developmental stages may also be critical to understand how cardiac resistance to β-adrenergic stimulation varies from the womb to adulthood (Iwasaki et al., 1990, Slotkin et al., 1995). Although many others stress/survival pathways could have been investigated in the present work, it is clear that cardiac and muscle cells in an early stage of differentiation have more intrinsic defenses. Finally, the results here obtained advice carefully planning when investigating drug-induced toxicity in a cell line model, since the differentiation state may not always mimic what occurs in an *in vivo* system.

5. Acknowledgements

Funded by Foundation for Science and Technology (FCT-Portugal): PEst-C/SAU/LA0001/2013-2014 (to CNC), PTDC/QUI/64358/2006 to PO (co-funded by FEDER through COMPETE program and by the Portuguese National Budget), and by fellowships SFRH/BD/ 41384/2007 (AB) and SFRH/BPD/31549/2006 (VS). MRW was

supported by BIO-IMAGing in research Innovation and Education (FP7-REGPOT-2010-1) grant. The funding agency had no role in data analysis or in the decision of publishing the manuscript.

6. Conflicts of interest

The authors report that they have no conflicts of interest.

6. References

Afanas'ev I. ROS and RNS signaling in heart disorders: could antioxidant treatment be successful? Oxid Med Cell Longev 2011; 2011: 293769.

Aoyagi T, Matsui T. Phosphoinositide-3 kinase signaling in cardiac hypertrophy and heart failure. Curr Pharm Des 2011; 17: 1818-24.

Basha RH, Priscilla DH. An in vivo and in vitro study on the protective effects of N-acetylcysteine on mitochondrial dysfunction in isoproterenol treated myocardial infarcted rats. Exp Toxicol Pathol 2013; 65: 7-14.

Benov L, Sztejnberg L, Fridovich I. Critical evaluation of the use of hydroethidine as a measure of superoxide anion radical. Free Radic Biol Med 1998; 25: 826-31.

Bradford MM. A rapid and sensitive method for the quantitation of microgram quantities of protein utilizing the principle of protein-dye binding. Anal Biochem 1976; 72: 248-54.

Branco AF, Pereira SL, Moreira AC, Holy J, Sardao VA, Oliveira PJ. Isoproterenol cytotoxicity is dependent on the differentiation state of the cardiomyoblast H9c2 cell line. Cardiovasc Toxicol 2011; 11: 191-203.

Branco AF, Sampaio SF, Moreira AC, Holy J, Wallace KB, Baldeiras I, et al. Differentiation-dependent doxorubicin toxicity on H9c2 cardiomyoblasts. Cardiovasc Toxicol 2012; 12: 326-40.

Carpi A, Menabo R, Kaludercic N, Pelicci P, Di Lisa F, Giorgio M. The cardioprotective effects elicited by p66(Shc) ablation demonstrate the crucial role of mitochondrial ROS formation in ischemia/reperfusion injury. Biochim Biophys Acta 2009; 1787: 774-80.

Chaitanya GV, Babu PP. Differential PARP cleavage: an indication of heterogeneous forms of cell death and involvement of multiple proteases in the infarct of focal cerebral ischemia in rat. Cell Mol Neurobiol 2009; 29: 563-73.

Chiong M, Wang ZV, Pedrozo Z, Cao DJ, Troncoso R, Ibacache M, et al. Cardiomyocyte death: mechanisms and translational implications. Cell Death Dis 2011; 2: e244.

Chung S, Dzeja PP, Faustino RS, Perez-Terzic C, Behfar A, Terzic A. Mitochondrial oxidative metabolism is required for the cardiac differentiation of stem cells. Nat Clin Pract Cardiovasc Med 2007; 4 Suppl 1: S60-7.

Comelli M, Domenis R, Bisetto E, Contin M, Marchini M, Ortolani F, et al. Cardiac differentiation promotes mitochondria development and ameliorates oxidative capacity in H9c2 cardiomyoblasts. Mitochondrion 2011; 11: 315-26.

Communal C, Singh K, Pimentel DR, Colucci WS. Norepinephrine stimulates apoptosis in adult rat ventricular myocytes by activation of the beta-adrenergic pathway. Circulation 1998; 98: 1329-34.

Cosentino F, Francia P, Camici GG, Pelicci PG, Luscher TF, Volpe M. Final common molecular pathways of aging and cardiovascular disease: role of the p66Shc protein. Arterioscler Thromb Vasc Biol 2008; 28: 622-8.

Di Lisa F, Carpi A, Giorgio V, Bernardi P. The mitochondrial permeability transition pore and cyclophilin D in cardioprotection. Biochim Biophys Acta 2011; 1813: 1316-22.

Diwan A, Dorn GW, 2nd. Decompensation of cardiac hypertrophy: cellular mechanisms and novel therapeutic targets. Physiology (Bethesda) 2007; 22: 56-64.

Fu JD, Yu HM, Wang R, Liang J, Yang HT. Developmental regulation of intracellular calcium transients during cardiomyocyte differentiation of mouse embryonic stem cells. Acta Pharmacol Sin 2006; 27: 901-10.

Fujita T, Ishikawa Y. Apoptosis in heart failure. -The role of the beta-adrenergic receptor-mediated signaling pathway and p53-mediated signaling pathway in the apoptosis of cardiomyocytes. Circ J 2011; 75: 1811-8.

Giorgio V, Soriano ME, Basso E, Bisetto E, Lippe G, Forte MA, et al. Cyclophilin D in mitochondrial pathophysiology. Biochim Biophys Acta 2010; 1797: 1113-8.

Gomez JP, Potreau D, Raymond G. Intracellular calcium transients from newborn rat cardiomyocytes in primary culture. Cell Calcium 1994; 15: 265-75.

Halestrap AP. A pore way to die: the role of mitochondria in reperfusion injury and cardioprotection. Biochem Soc Trans 2010; 38: 841-60.

Harris EJ. The uptake and release of calcium by heart mitochondria. Biochem J 1977; 168: 447-56.

Hou Q, Hsu YT. Bax translocates from cytosol to mitochondria in cardiac cells during apoptosis: development of a GFP-Bax-stable H9c2 cell line for apoptosis analysis. Am J Physiol Heart Circ Physiol 2005; 289: H477-87.

Houghton P, Fang R, Techatanawat I, Steventon G, Hylands PJ, Lee CC. The sulphorhodamine (SRB) assay and other approaches to testing plant extracts and

derived compounds for activities related to reputed anticancer activity. Methods 2007; 42: 377-87.

Iwasaki T, Takino Y, Suzuki T. Effects of isoproterenol on the developing heart in rats. Jpn Circ J 1990; 54: 109-16.

Izem-Meziane M, Djerdjouri B, Rimbaud S, Caffin F, Fortin D, Garnier A, et al. Catecholamine-induced cardiac mitochondrial dysfunction and mPTP opening: protective effect of curcumin. Am J Physiol Heart Circ Physiol 2012; 302: H665-74.

Lebiedzinska M, Karkucinska-Wieckowska A, Wojtala A, Suski JM, Szabadkai G, Wilczynski G, et al. Disrupted ATP synthase activity and mitochondrial hyperpolarisation-dependent oxidative stress is associated with p66Shc phosphorylation in fibroblasts of NARP patients. Int J Biochem Cell Biol 2013; 45: 141-50.

Leblais V, Jo SH, Chakir K, Maltsev V, Zheng M, Crow MT, et al. Phosphatidylinositol 3-kinase offsets cAMP-mediated positive inotropic effect via inhibiting Ca2+ influx in cardiomyocytes. Circ Res 2004; 95: 1183-90.

Lee YK, Ng KM, Lai WH, Chan YC, Lau YM, Lian Q, et al. Calcium homeostasis in human induced pluripotent stem cell-derived cardiomyocytes. Stem Cell Rev 2011; 7: 976-86.

Li Q, Zhou LY, Gao GF, Jiao JQ, Li PF. Mitochondrial network in the heart. Protein Cell 2012; 3: 410-8.

Mann DL, Kent RL, Parsons B, Cooper Gt. Adrenergic effects on the biology of the adult mammalian cardiocyte. Circulation 1992; 85: 790-804.

Marella M, Seo BB, Matsuno-Yagi A, Yagi T. Mechanism of cell death caused by complex I defects in a rat dopaminergic cell line. J Biol Chem 2007; 282: 24146-56.

Menard C, Pupier S, Mornet D, Kitzmann M, Nargeot J, Lory P. Modulation of L-type calcium channel expression during retinoic acid-induced differentiation of H9C2 cardiac cells. J Biol Chem 1999; 274: 29063-70.

Metzger JM, Lin WI, Samuelson LC. Transition in cardiac contractile sensitivity to calcium during the in vitro differentiation of mouse embryonic stem cells. J Cell Biol 1994; 126: 701-11.

Mildaziene V, Baniene R, Nauciene Z, Marcinkeviciute A, Morkuniene R, Borutaite V, et al. Ca2+ stimulates both the respiratory and phosphorylation subsystems in rat heart mitochondria. Biochem J 1996; 320 (Pt 1): 329-34.

Minakawa M, Takeuchi K, Ito K, Tsushima T, Fukui K, Takaya S, et al. Restoration of sarcoplasmic reticulum protein level by thyroid hormone contributes to partial improvement of myocardial function, but not to glucose metabolism in an early failing heart. Eur J Cardiothorac Surg 2003; 24: 493-501.

Morten KJ, Ackrell BA, Melov S. Mitochondrial reactive oxygen species in mice lacking superoxide dismutase 2: attenuation via antioxidant treatment. J Biol Chem 2006; 281: 3354-9.

Nichtova Z, Novotova M, Kralova E, Stankovicova T. Morphological and functional characteristics of models of experimental myocardial injury induced by isoproterenol. Gen Physiol Biophys 2012; 31: 141-51.

Ogata Y, Takahashi M. Bcl-xL as an antiapoptotic molecule for cardiomyocytes. Drug News Perspect 2003; 16: 446-52.

Pagano M, Naviglio S, Spina A, Chiosi E, Castoria G, Romano M, et al. Differentiation of H9c2 cardiomyoblasts: The role of adenylate cyclase system. J Cell Physiol 2004; 198: 408-16.

Pereira CV, Nadanaciva S, Oliveira PJ, Will Y. The contribution of oxidative stress to drug-induced organ toxicity and its detection in vitro and in vivo. Expert Opin Drug Metab Toxicol 2012; 8: 219-37.

Pereira SL, Ramalho-Santos J, Branco AF, Sardao VA, Oliveira PJ, Carvalho RA. Metabolic remodeling during H9c2 myoblast differentiation: relevance for in vitro toxicity studies. Cardiovasc Toxicol 2011; 11: 180-90.

Rong Y, Distelhorst CW. Bcl-2 protein family members: versatile regulators of calcium signaling in cell survival and apoptosis. Annu Rev Physiol 2008; 70: 73-91.

San Martin N, Cervera AM, Cordova C, Covarello D, McCreath KJ, Galvez BG. Mitochondria determine the differentiation potential of cardiac mesoangioblasts. Stem Cells 2011; 29: 1064-74.

Sardao VA, Oliveira PJ, Holy J, Oliveira CR, Wallace KB. Doxorubicin-induced mitochondrial dysfunction is secondary to nuclear p53 activation in H9c2 cardiomyoblasts. Cancer Chemother Pharmacol 2009; 64: 811-27.

Schmelter M, Ateghang B, Helmig S, Wartenberg M, Sauer H. Embryonic stem cells utilize reactive oxygen species as transducers of mechanical strain-induced cardiovascular differentiation. FASEB J 2006; 20: 1182-4.

Schmidt U, Hajjar RJ, Kim CS, Lebeche D, Doye AA, Gwathmey JK. Human heart failure: cAMP stimulation of SR Ca(2+)-ATPase activity and phosphorylation level of phospholamban. Am J Physiol 1999; 277: H474-80.

Serafim TL, Oliveira PJ, Sardao VA, Perkins E, Parke D, Holy J. Different concentrations of berberine result in distinct cellular localization patterns and

cell cycle effects in a melanoma cell line. Cancer Chemother Pharmacol 2008; 61: 1007-18.

Slotkin TA, Lappi SE, Seidler FJ. Beta-adrenergic control of c-fos expression in fetal and neonatal rat tissues: relationship to cell differentiation and teratogenesis. Toxicol Appl Pharmacol 1995; 133: 188-95.

Sun H, Oudit GY, Ramirez RJ, Costantini D, Backx PH. The phosphoinositide 3-kinase inhibitor LY294002 enhances cardiac myocyte contractility via a direct inhibition of Ik,slow currents. Cardiovasc Res 2004; 62: 509-20.

Wang M, Sun GB, Sun X, Wang HW, Meng XB, Qin M, et al. Cardioprotective effect of salvianolic acid B against arsenic trioxide-induced injury in cardiac H9c2 cells via the PI3K/Akt signal pathway. Toxicol Lett 2013; 216: 100-7.

Zhang GX, Kimura S, Nishiyama A, Shokoji T, Rahman M, Yao L, et al. Cardiac oxidative stress in acute and chronic isoproterenol-infused rats. Cardiovasc Res 2005; 65: 230-8.

Zhang X, Szeto C, Gao E, Tang M, Jin J, Fu Q, et al. Cardiotoxic and Cardioprotective Features of Chronic beta-Adrenergic Signaling. Circ Res 2013; 112: 498-509.

Zhang Y, Kohler K, Xu J, Lu D, Braun T, Schlitt A, et al. Inhibition of p53 after acute myocardial infarction: reduction of apoptosis is counteracted by disturbed scar formation and cardiac rupture. J Mol Cell Cardiol 2011; 50: 471-8.

Zheltukhin AO, Chumakov PM. Constitutive and induced functions of the p53 gene. Biochemistry (Mosc) 2010; 75: 1692-721.

Zhou P, Zhao YT, Guo YB, Xu SM, Bai SH, Lakatta EG, et al. Beta-adrenergic signaling accelerates and synchronizes cardiac ryanodine receptor response to a single L-type Ca2+ channel. Proc Natl Acad Sci U S A 2009; 106: 18028-33.

Zorov DB, Juhaszova M, Sollott SJ. Mitochondrial ROS-induced ROS release: an update and review. Biochim Biophys Acta 2006; 1757: 509-17.

8. Legends for figures

Figure 1 – H9c2 alterations after incubation with ISO for 48 hours. A) Effect of the differentiation process on β1- and β2-AR content. β1-AR (A) and β2-AR (B) protein content was evaluated by Western Blotting (see Materials and Methods) and identified as bands of approximately 70 and 50 kDa, respectively. H9c2 cells were differentiated in the presence and in absence of 1μM RA and total extracts were collected. Ponceau labeling represents the loading control and was used to normalize data. Data represent the mean±SEM of 3 independent experiments (*) $p<0.05$ versus undifferentiated H9c2 cells.

To investigate ISO effects on cell morphology and mitochondrial polarization by epifluorescence microscopy, H9c2 cells were cultured in high-serum media (10% FBS, C), low serum media (1% FBS, D) and low serum media daily supplemented with RA (1% FBS + 1 μM RA, D). H9c2 cells were incubated with 10, 20, 50, 100 and 150 μM of ISO and labeled with Hoechst 33342 (nuclei, blue fluorescence) and TMRM (mitochondria, red fluorescence). Epifluorescence microscopy images are representative from 3 different cell preparations. White arrows indicate cells with apoptotic nuclei

(Hoechst column) or cells with depolarized mitochondria (TMRM column). The white bar represents 60 μm.

Figure 2 - Alteration of cytosolic calcium and cAMP after ISO incubation. Evaluation of intracellular calcium on undifferentiated and differentiated cells was performed under untreated and after 2, 3 and 6 hours of ISO treatment (A). Intracellular calcium content was evaluated by using Fluo-4-AM, as described in the Materials and Methods section. The data shows the means±SEM, (*) significant difference vs. cells in 10% FBS (left) or to the respective control (right) ($p<0.05$). (B) Evaluation of intracellular cAMP levels. The data shows means±SEM, (*) significant differences vs. cells in 10% FBS (left) or to the respective control (right) ($p<0.05$).

Figure 3 - Evaluation of mitochondria polarization and superoxide anion in H9c2 cells. Quantitative evaluation of TMRM (A-E) and MitoSox (F-J) fluorescence, as measured by flow cytometry. Undifferentiated and differentiated cells in the presence or absence of RA were treated with ISO for 1, 3, 6 and 48 hours (panels B-E and G-J), as described in the Materials and Methods section. Panels A and F represent TMRM and MitoSox fluorescence under untreated conditions. For MitoSox experiments, cells were incubated with 9 μM rotenone for 1 hour to determine the maximal value for superoxide anion detection. For panels G-J, the values obtained are normalized for the respective rotenone control value, to compensate for possible differences in maximal superoxide production. Data are means of 4 (for TMRM-labeling assay) or 5 (for MitoSox-labeling assay) independent experiments±SEM. Panels E, I and J, (*) $p<0.05$ vs. respective control; Panel F, (*) $p<0.05$ vs. no rotenone; (#) $p<0.05$ vs. 10% FBS cells.

Figure 4 - Evaluation of mitochondrial alterations after ISO treatment. Mitochondrial oxidative phosphorylation subunits were identified by Western Blotting after H9c2 undifferentiated and differentiated cells (in presence and in absence of RA) were treated with 50 and 100 μM of ISO for 48 hours. The antibodies used detected the proteins NDUFB8 (subunit of complex I), 30kDa subunit (complex II) and ATP synthase subunit alpha. Ponceau labeling was used as loading control. The results are representative of the means±SEM of 4 separate assays. (*) $p<0.05$ vs. respective control.

Figure 5 - Isoproterenol induces toxicity responses in H9c2 cells. Bcl-xL (A), SOD2 (B), cyclophilin F (C), p53 (D) total and Ser36phosphorylated-p66Shc (E) protein content were measured by Western Blotting (see Materials and Methods). H9c2 cells in the different treatment groups were incubated with ISO for 48hours and total cellular extracts were collected. Ponceau labeling and non-phosphorylated p66Shc labeling served to normalize protein loading. Data represent the mean±SEM of 5 independent experiments. (*) $p<0.05$ vs. respective control, same differentiation group.

Figure 6 - p53 and oxidative stress involvement during ISO toxicity on H9c2 cells. The sulforhodamine B assay was performed to investigate if the p53 inhibitor pifithrin-alpha (A) or the antioxidant NAC (B) prevented H9c2 cell death caused by ISO. Undifferentiated myoblasts were incubated with ISO for 3 (A) or 4 (B) days, while differentiated cells (in presence or absence of RA) were incubated with ISO for 48 hours. Cells were pre-incubated for 30 minutes with 30 μM of pifithrin-alpha or for 2

hours with 100 μM NAC. Data represent the mean±SEM of 4 (for NAC) and 5 (for pifithrin-alpha) independent experiments (*) $P<0.05$ undifferentiated cells vs. the same concentration used on differentiated cells.

Figure 7 - PI3K/Akt pathway role on ISO-induced toxicity. (A) H9c2 undifferentiated and differentiated cells were incubated with ISO for 48 hours and samples were collected as described in Materials and Methods section. Total Akt and the phosphorylated form in serine 437 were identified by Western Blotting. Ponceau labeling was used as loading control. Data represent the mean ± SEM of 4 independent experiments (*) $P<0.05$ versus respective control for the same differentiation state group. (C) Undifferentiated and differentiated H9c2 cells were pre-incubated with the PI3K/Akt pathway inhibitor LY294002 1 hour prior the addition of 50 or 100μM of ISO. Differentiated cell number was analyzed after 24 hours and undifferentiated cells after 48 hours of ISO treatment, by using the SRB assay method. Data represent the mean±SEM of 4 independent experiments (*) $P<0.05$ of undifferentiated cells vs. the same concentration used on differentiated cells (D) Confocal microscopy images of differentiated H9c2 cells in the presence and in absence of RA incubated with ISO after pre-incubation with LY294002 by using the same protocol as in (C). Preparations were incubated with Mitotracker Red (to label mitochondria) and DAPI (to label nuclei). White bar corresponds to 60μm.

Figure 8 - Caspase 3-like activity in H9c2 cells exposed to ISO and effect of caspase inhibition. (A) The full length caspase 3 and caspase 3-resulting fragments were determined by Western Blotting and identified as bands with 35 and 19/17 kDa, respectively. Ponceau labeling was used as loading control and to normalize the results

of determining the cleaved-caspase 3 content. Data represent the mean±SEM of 3 independent experiments (*) P<0.05 versus respective control for the same differentiation state group. (B) By using a colorimetric assay, undifferentiated and differentiated H9c2 cells exposed to ISO were analyzed in order to measure caspase 3-like activity. Data represent the mean ± SEM of 4 independent experiments (*) P<0.05 versus respective control for the same differentiation state group. Data represent the mean±SEM of 3 independent experiments (*) P<0.05 vs. control.

Figure 9 – Representative diagram of the main findings of the present study. Before ISO treatment, levels of SOD2, Bcl-xL and Cycl. D were increased in undifferentiated H9c2 cells; on the other hand, a decrease in β_1-adrenergic receptors, cAMP and Bcl-xL protein, as well as an increase in intracellular calcium, oxidative stress, p53, p66Shc, phosphorylated AKT and in caspase 3 activity were measured.

Distinct responses to ISO were observed in undifferentiated and differentiated H9c2 cells. We propose that RA-differentiated cells are more susceptible to ISO, with calcium being an important mediator of the difference between the different groups of cells. Increased cytosolic calcium is observed in differentiated vs. undifferentiated is observed, which may lead to mitochondrial alterations, leading to triggering of apoptosis. These alterations may include increased mitochondrial generation of superoxide anion and membrane depolarization. Mitochondrial oxidative stress may also increase due to cytosolic redox-dependent activation of the p66Shc signaling pathway, which may inhibit any potential adaptative increase in superoxide dismutase 2 (SOD2). The lack of p66Shc activation in undifferentiated cells may explain the observed increase in SOD2, which may act to decrease mitochondrial oxidative stress and inhibit apoptotic signaling. Mitochondrial oxidative stress in differentiated cells may also lead to damage to oxidative phosphorylation subunits, while global oxidative

stress in the cell may damage DNA, resulting to the activation of p53 and triggering of mitochondrial-dependent apoptosis mediated by the pro-apoptotic protein Bax. Ultimately, caspase 3 is activated downstream and apoptosis in differentiated cells enters a point of no return. NAC (n-acetylcysteine) and pifithrin-alpha (Pifα) inhibit oxidative stress and p53 activation respectively in differentiated cells. Activation of the AKT pathway in undifferentiated and differentiated cells acts to possibly prevent induction of apoptosis caused by ISO, although it may be acting less effectively in the former group of cells. While an increase in Bcl-xL (shown in this work) and Bcl-2 (Branco et al., 2011) antagonize the induction of the mitochondrial pathway of apoptosis, the role of cyclophilin-D (Cycl.D) is less clear.

Highlights

Isoproterenol (ISO) toxicity depends on muscle cell differentiation

ISO triggers different toxicity pathways on differentiated H9c2 myoblasts

Undifferentiated H9c2 cells challenged with ISO up-regulated SOD2 and Bcl-xL

Differentiation of H9c2 is associated with differential regulation of stress responses, which regulates ISO effects

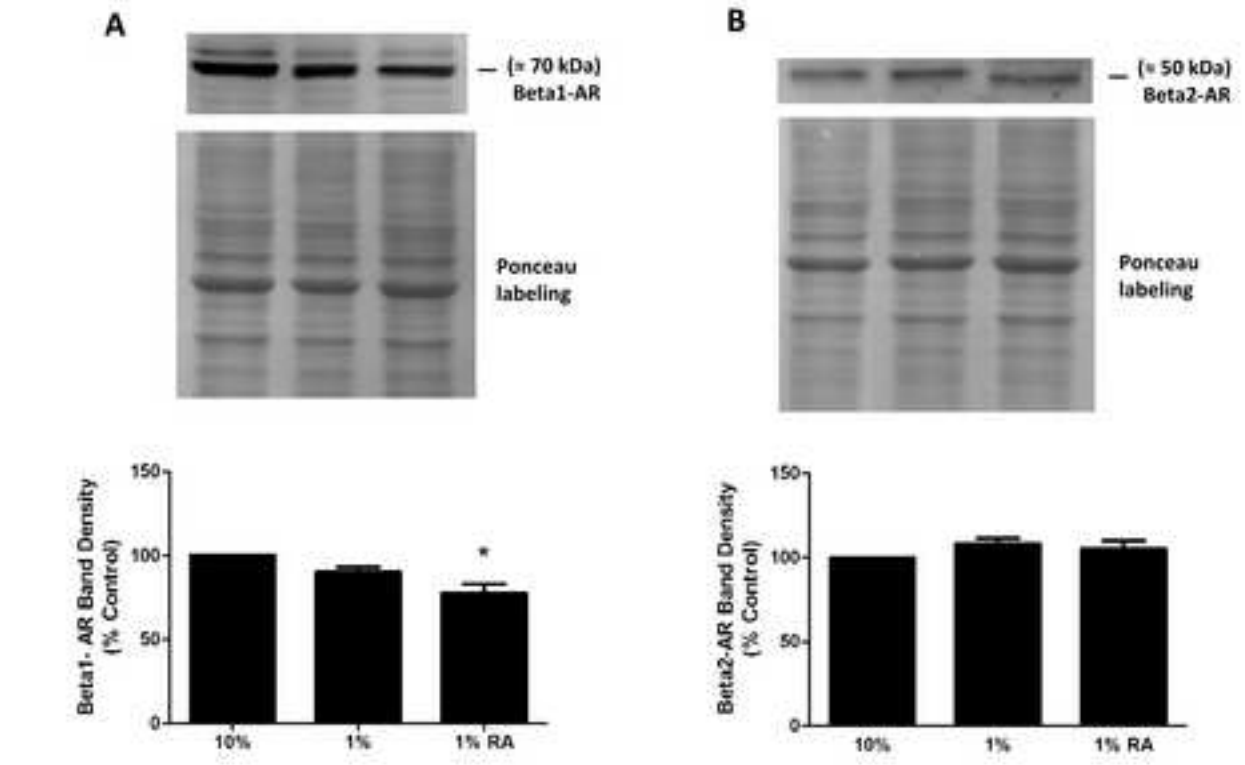

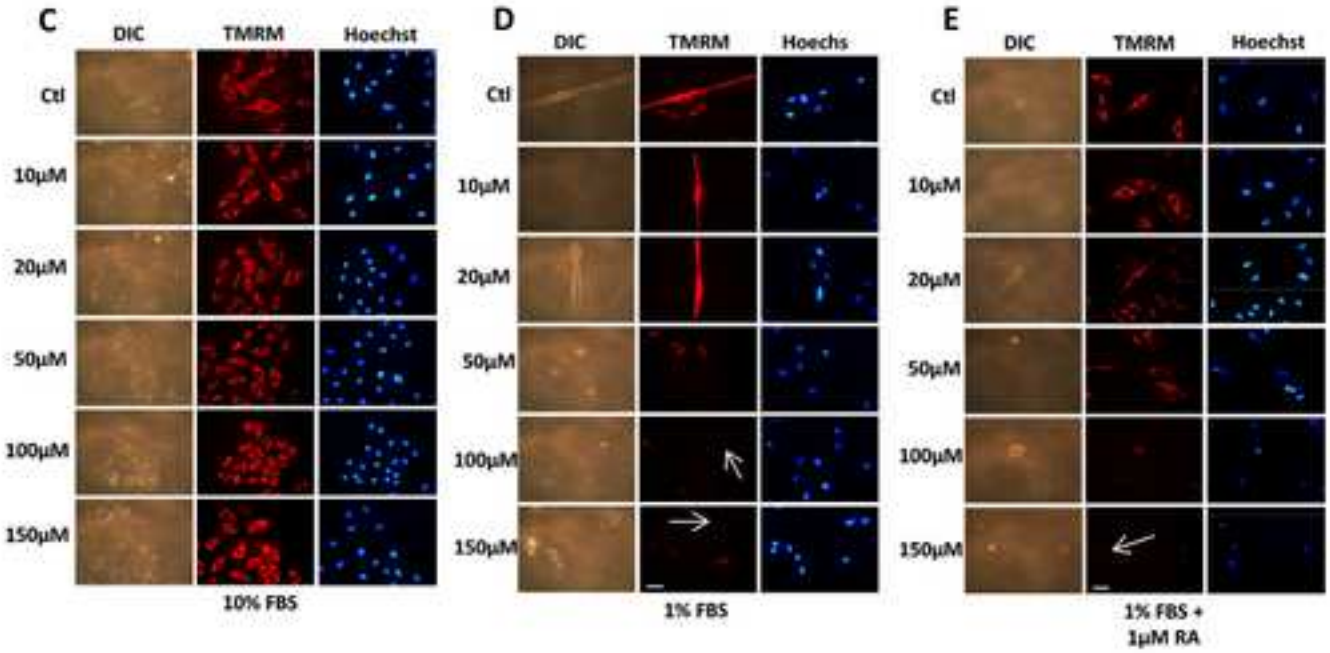

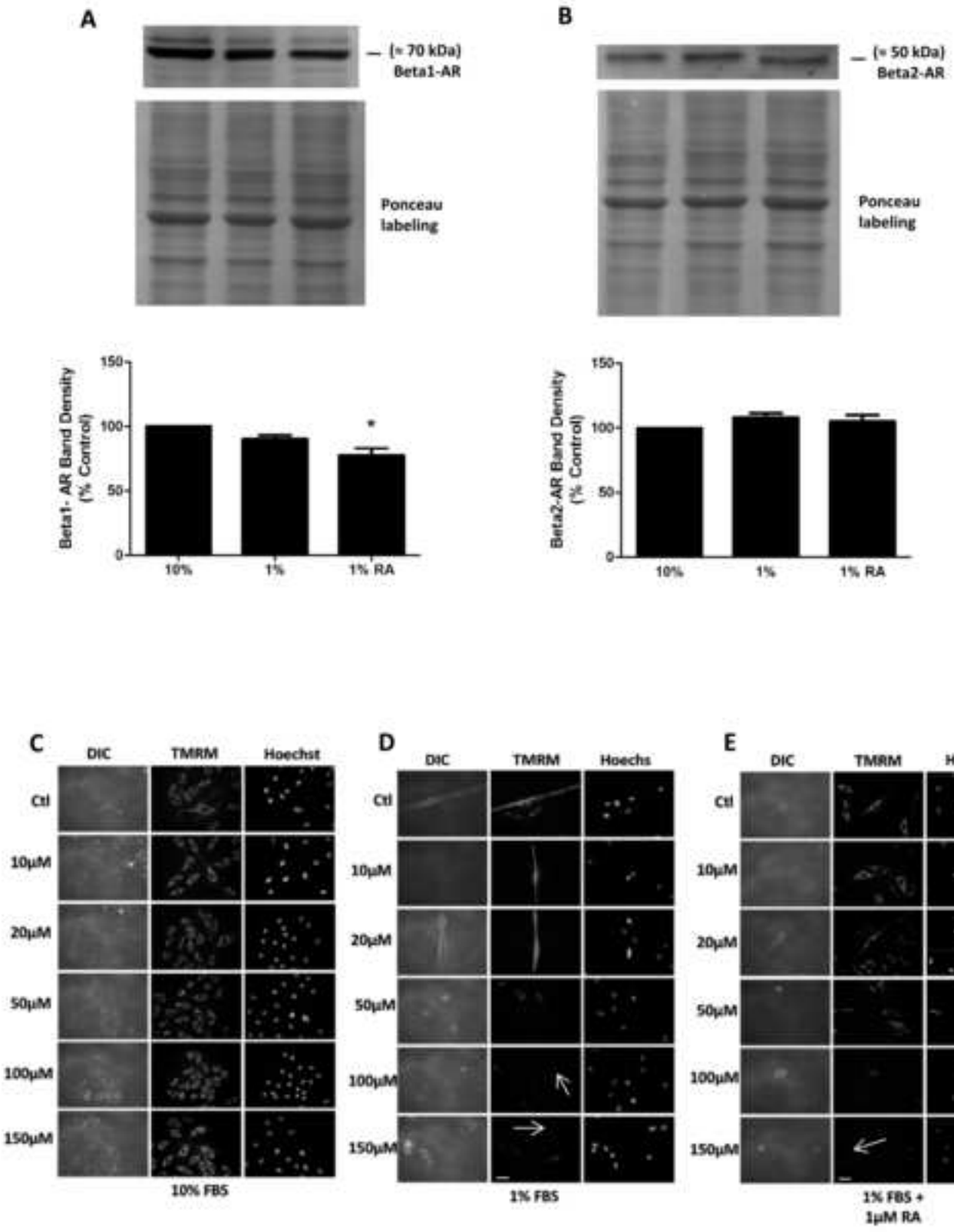

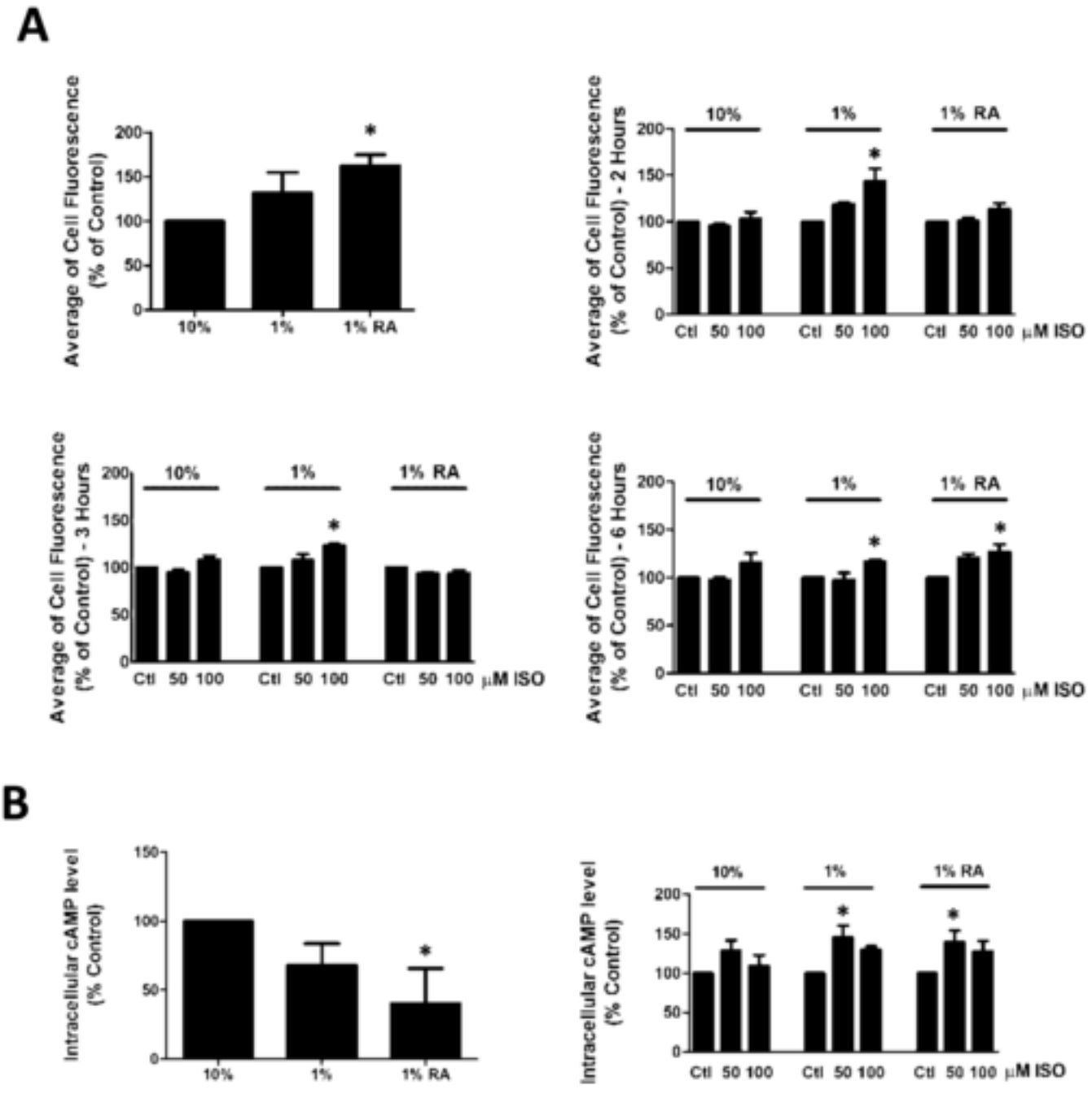

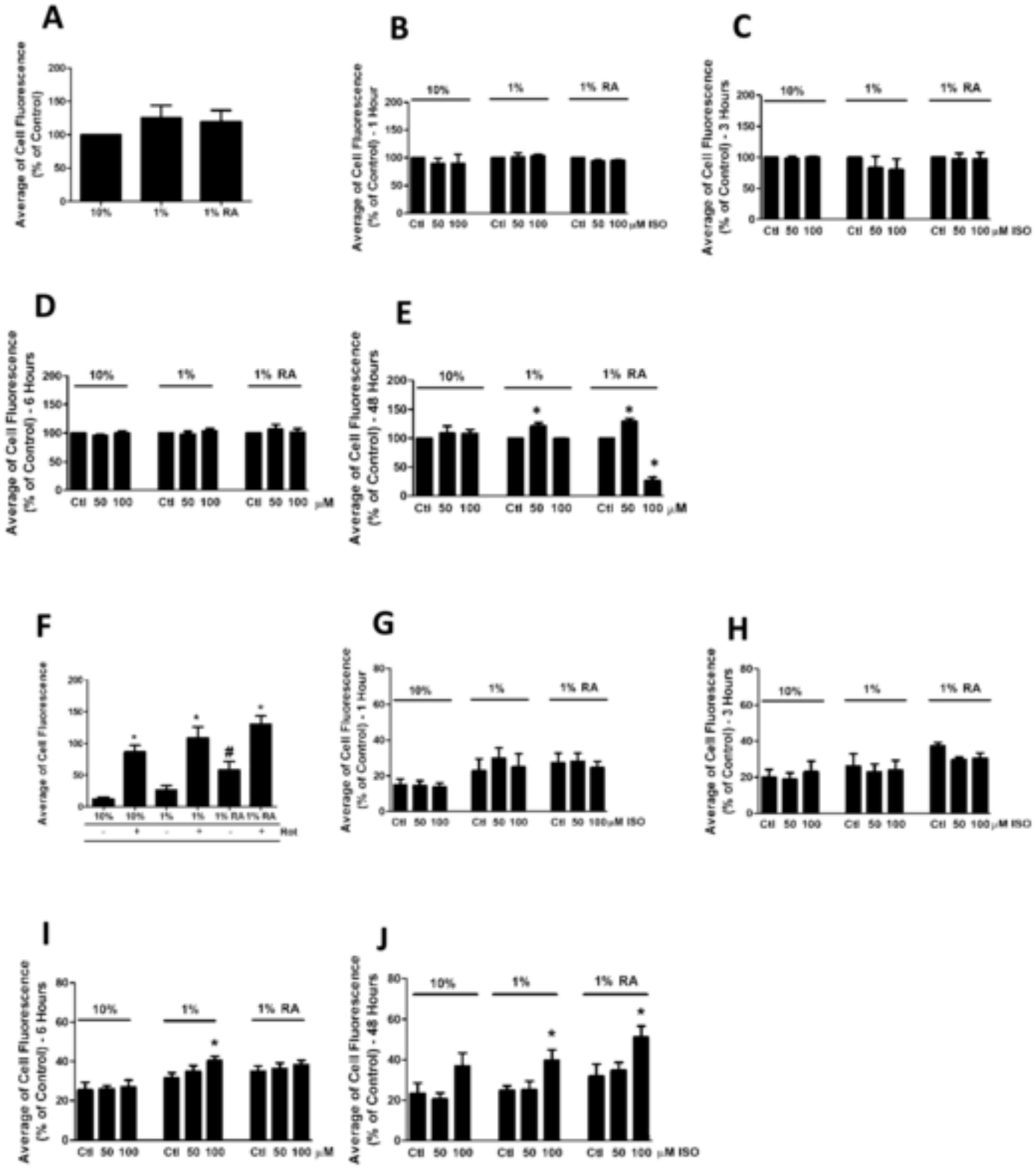

Figure 4

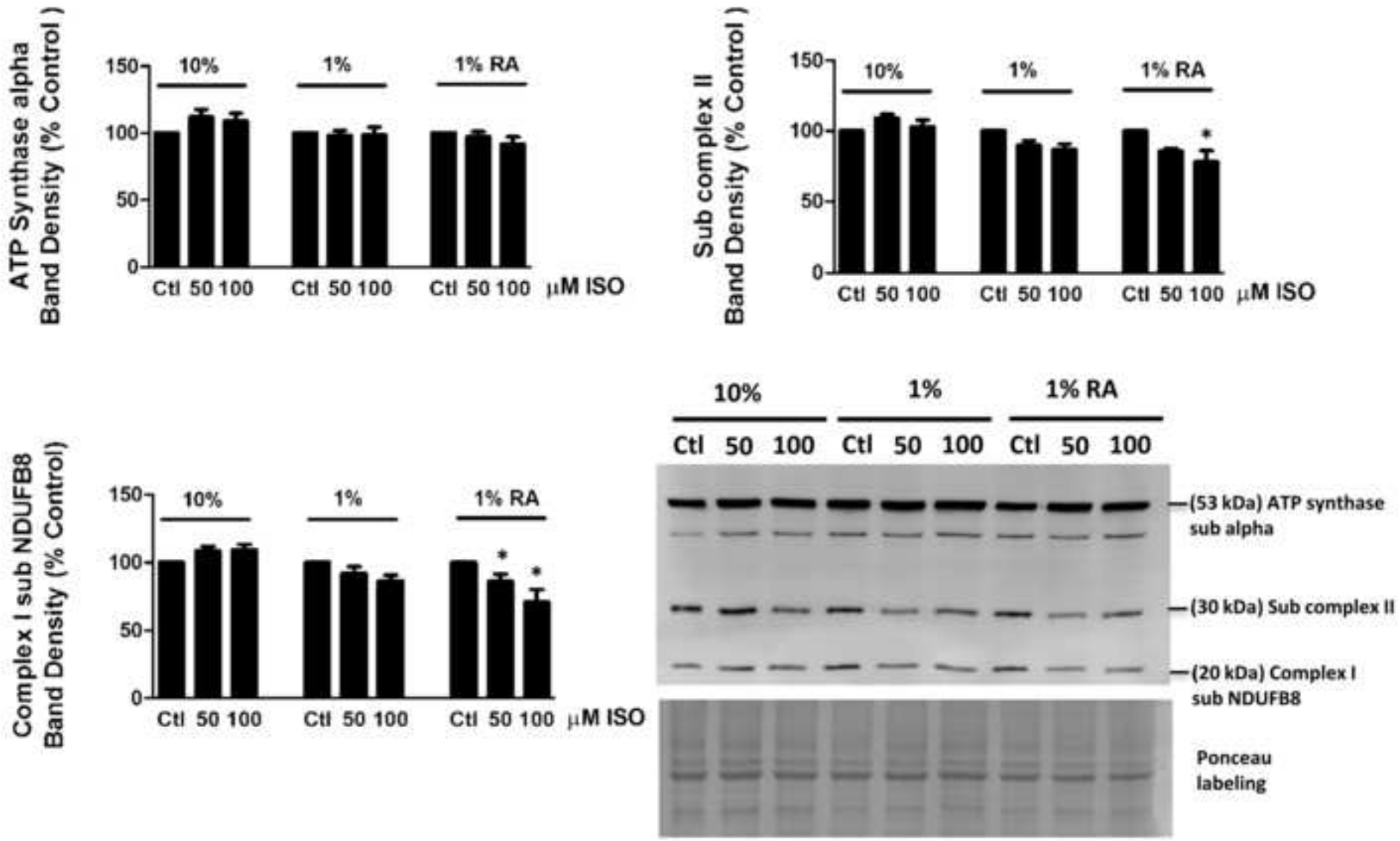
ATP Synthase alpha
Band Density (% Control)
150
100
50
0
10%
1%
1% RA
Ctl 50 100
Ctl 50 100
Ctl 50 100
µM ISO
Sub complex II
Band Density (% Control)
150
100
50
0
10%
1%
1% RA
*
Ctl 50 100
Ctl 50 100
Ctl 50 100
µM ISO
Complex I sub NDUFB8
Band Density (% Control)
150
100
50
0
10%
1%
1% RA
*
*
Ctl 50 100
Ctl 50 100
Ctl 50 100
µM ISO
10%
1%
1% RA
Ctl 50 100 Ctl 50 100 Ctl 50 100
(53 kDa) ATP synthase sub alpha
(30 kDa) Sub complex II
(20 kDa) Complex I sub NDUFB8
Ponceau labeling

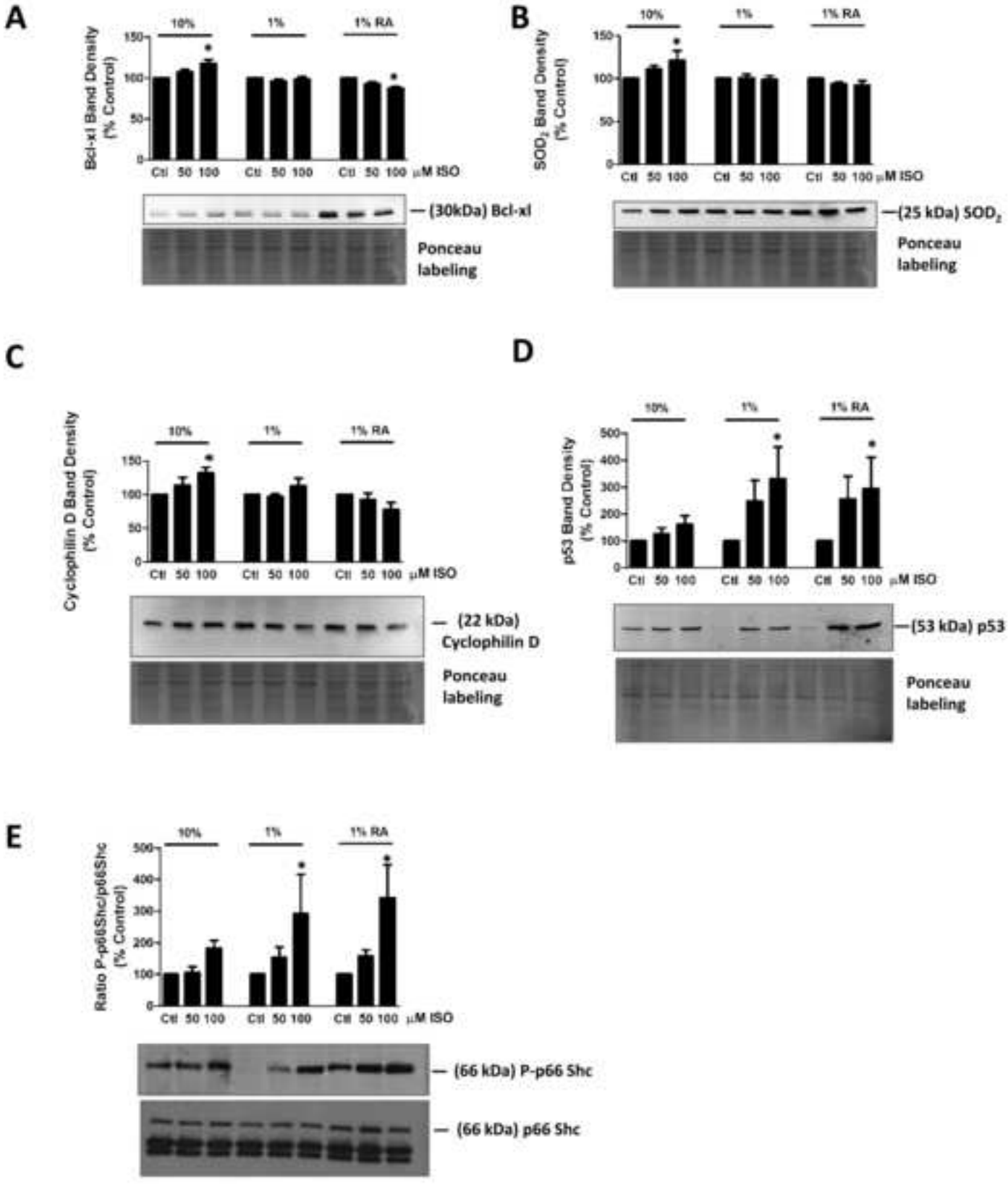

Figure 6

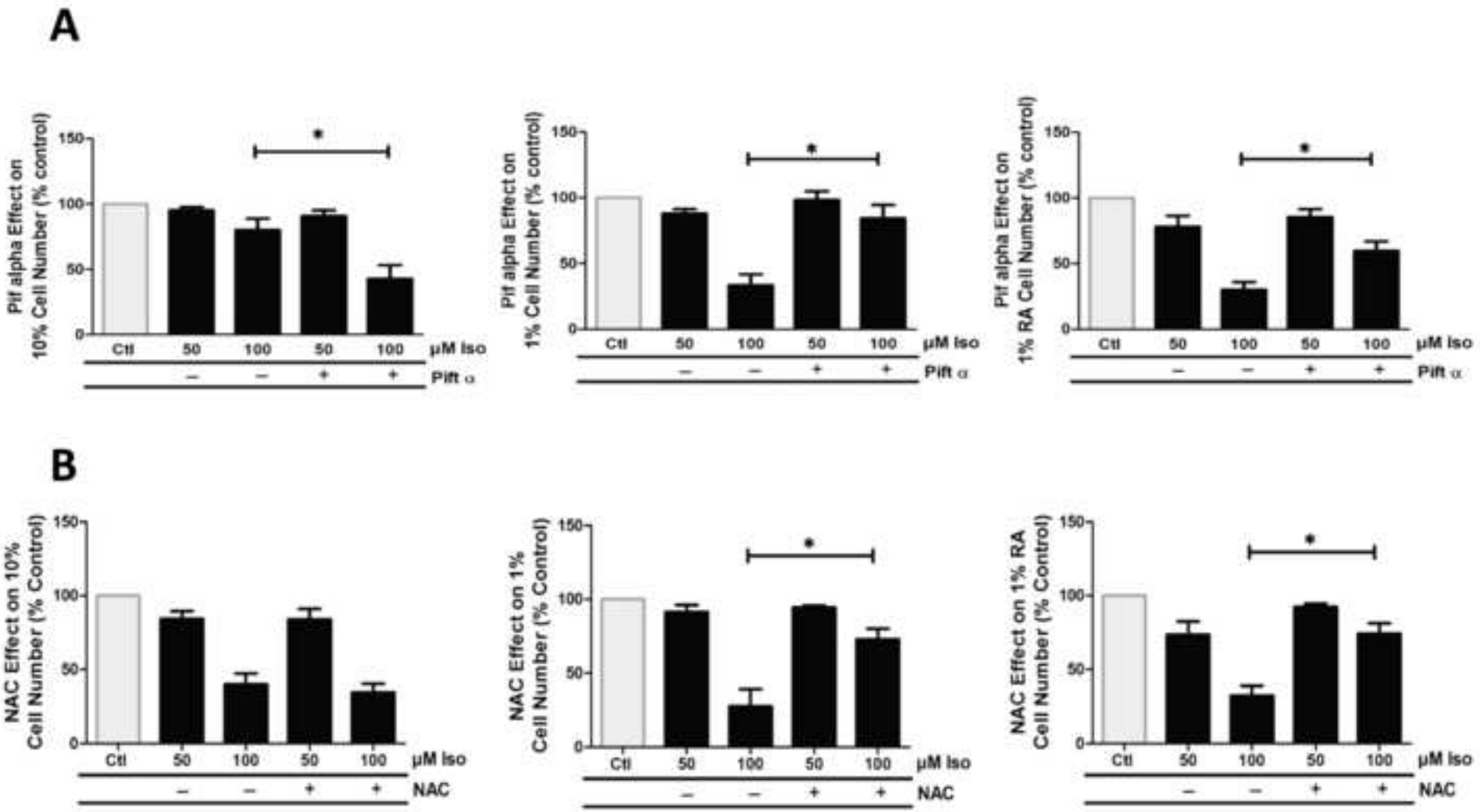
A
Pif alpha Effect on 10% Cell Number (% control)
Pif alpha Effect on 1% Cell Number (% control)
Pif alpha Effect on 1% RA Cell Number (% control)
150
100
50
0
*
Ctl
50
100
50
100
µM Iso
–
–
+
+
Pift α
B
NAC Effect on 10% Cell Number (% Control)
NAC Effect on 1% Cell Number (% Control)
NAC Effect on 1% RA Cell Number (% Control)
NAC

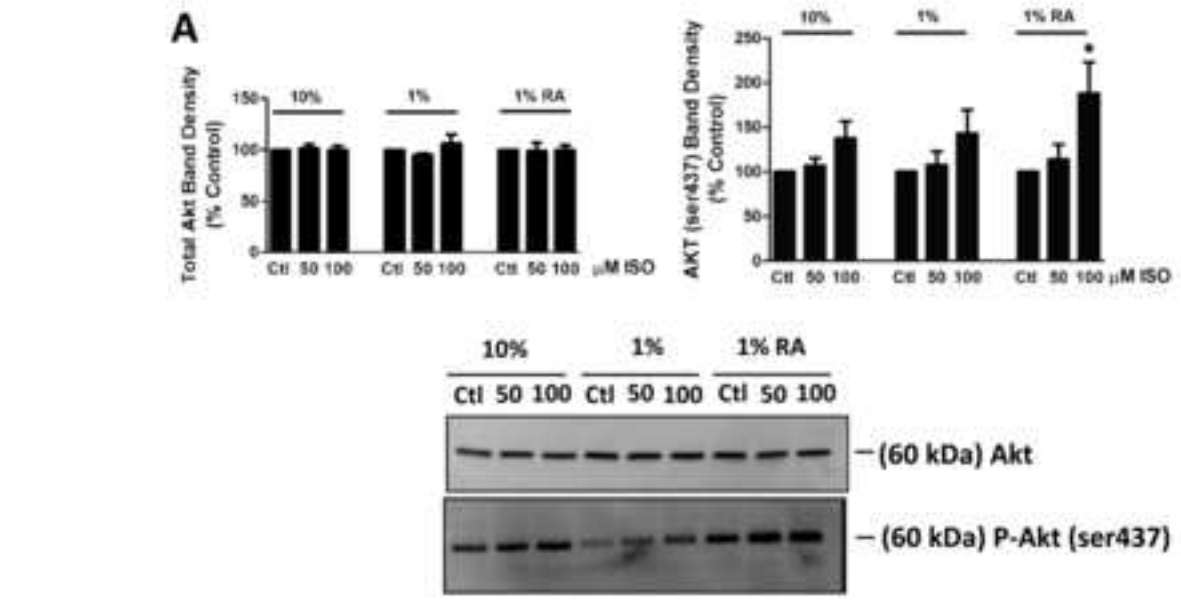

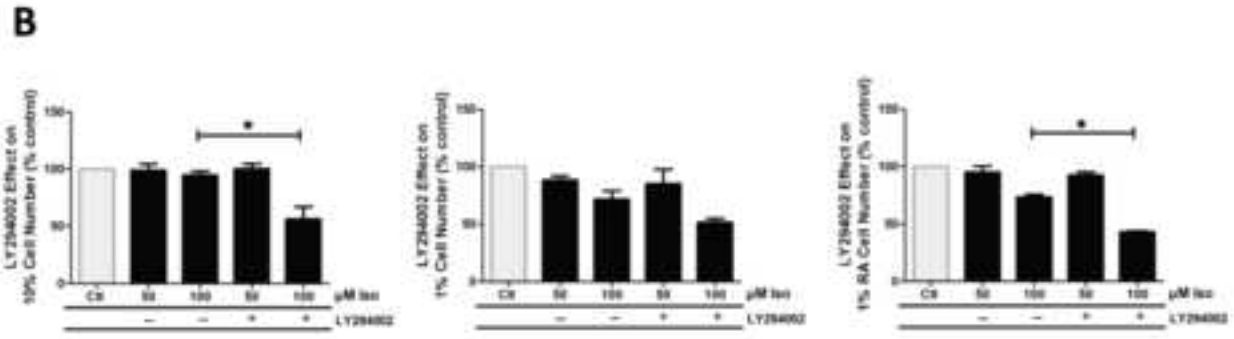

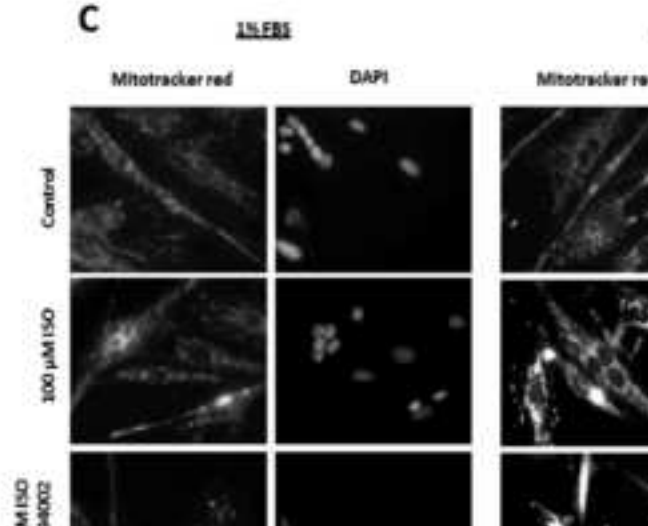

Figure 8

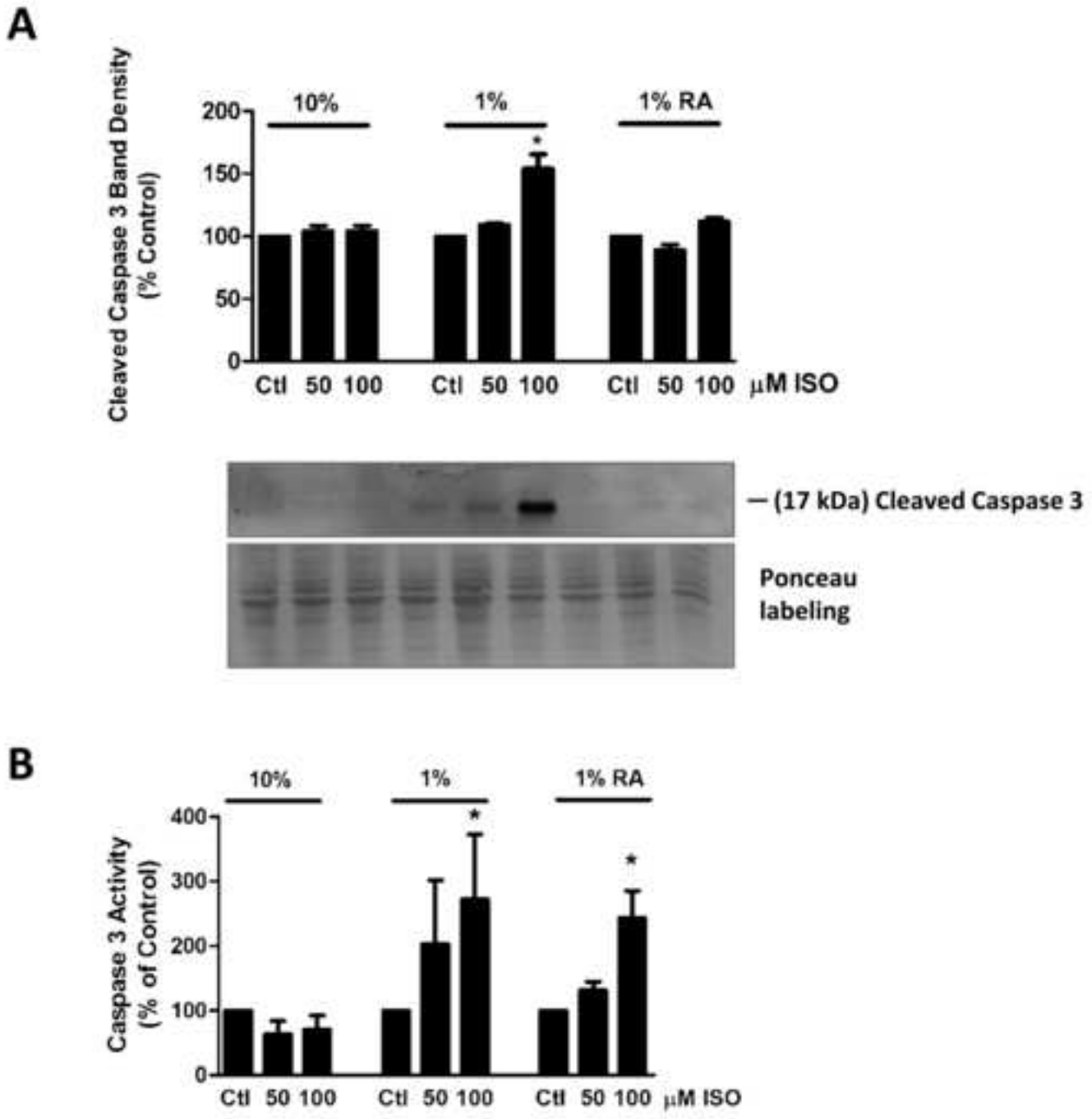
A
Cleaved Caspase 3 Band Density (% Control)
200
150
100
50
0
10%
1%
1% RA
*
Ctl 50 100 Ctl 50 100 Ctl 50 100 μM ISO
— (17 kDa) Cleaved Caspase 3
Ponceau labeling
B
Caspase 3 Activity (% of Control)
400
300
200
100
0
10%
1%
1% RA
*
*
Ctl 50 100 Ctl 50 100 Ctl 50 100 μM ISO